Structural Engineering and Mechanics, Vol. 6, No. 8 (1998) 939-953
DOI: http://dx.doi.org/10.12989/sem.1998.6.8.939

Vibration, buckling and dynamic stability of a cantilever rectangular plate subjected to in-plane force

Kazuo Takahashi†, Mincharn Wu‡ and Satoshi Nakazawa‡

Department of Civil Engineering, Nagasaki University, 1-14 Bunkyo-machi, Nagasaki 852-8131, Japan

Abstract. Vibration, buckling and dynamic stability of a cantilever rectangular plate subjected to an in-plane sinusoidally varying load applied along the free end are analyzed. The thin plate small deflection theory is used. The Rayleigh-Ritz method is employed to solve vibration and buckling of the plate. The dynamic stability problem is solved by using the Hamilton principle to drive time variables. The resulting time variables are solved by the harmonic balance method. Buckling properties and natural frequencies of the plate are shown at first. Unstable regions are presented for various loading conditions. Simple parametric resonances and combination resonances with sum type are obtained for various loading conditions, static load and damping.

Key words: dynamic stability; cantilever rectangular plate; vibration; buckling.

1. Introduction

The dynamic stability of a thin rectangular plate has been studied by many researchers (Bolotin 1964, Yamaki and Nagai 1975). In these studies, however, a uniformly distributed load has been treated under relatively simple boundary conditions and mainly simple parametric resonances have been considered. The buckling and dynamic stability of a thin beam subjected to in-plane load are analyzed when the aspect ratio is large (Column Research Committee of Japan 1971). However, when the aspect ratio is small, the plate theory must be applied to the problem. The dynamic stability of a rectangular plate subjected to in-plane bending load such as a concentrated load or a distributed load, remains to be considered.

Theoretical solutions are reported for the dynamic stability of a rectangular plate under linearly distributed periodic loads applied along two opposite edges by the author (Takahashi and Konishi 1988). In this paper, theoretical solutions are reported for the dynamic stability of a cantilever rectangular plate under in-plane bending loads applied along free ends. The problem is solved by using the Hamilton principal and the harmonic balance method described by the authors (Takahashi 1982, 1981).

After presenting the problem in the eigenvalue form, numerical results are presented, first,

† Professor
‡ Graduate Student

for buckling properties and natural frequencies of the plate and second, for dynamic unstable regions of the cantilever rectangular plate with various loading conditions along the edge.

2. Basic equations

Assume that a cantilever rectangular plate with length a, width b and thickness h is subjected to in-plane bending loads. A cartesian co-ordinate system (x, y) is introduced as shown in Fig. 1. The in-plane forces N_x, N_y and N_{xy} due to static load q_0 and periodic dynamic load $q_t \cos\Omega t$ are obtained by two dimensional theory of elasticity, as follows

$$\begin{aligned} N_x &= (p_0 + p_t \cos\Omega t)\cdot f_1(x, y) \\ N_y &= (p_0 + p_t \cos\Omega t)\cdot f_2(x, y) \\ N_{xy} &= (p_0 + p_t \cos\Omega t)\cdot f_3(x, y) \end{aligned} \tag{1}$$

in which p_0 and p_t are the amplitudes of the static and dynamic loads, respectively, Ω is the radian excitation frequency and, $f_1(x, y)$, $f_2(x, y)$, and $f_3(x, y)$ are functions characterized by the distribution of the in-plane bending load as shown in Fig. 2. That is,

Case I: concentrated load along the free end $x=a$;

Case II: uniformly distributed load along the free end $y=0$;

Case III: triangularly distributed load along the free end $y=0$.

In-plane forces, N_x, N_y and N_{xy} are shown in Appendix A for the three cases.

It is assumed that effects of longitudinal and rotatory inertia forces and transverse shear can be neglected.

Strain energy V, strain energy due to in-plane forces U and kinetic energy T of the plate are given by

$$V = \frac{1}{2} D \iint_A \left\{ (\nabla^2 w)^2 - 2(1-\nu)\left[\frac{\partial^2 w}{\partial x^2}\frac{\partial^2 w}{\partial y^2} - \left(\frac{\partial^2 w}{\partial x \partial y} \right)^2 \right] \right\} dxdy \tag{2}$$

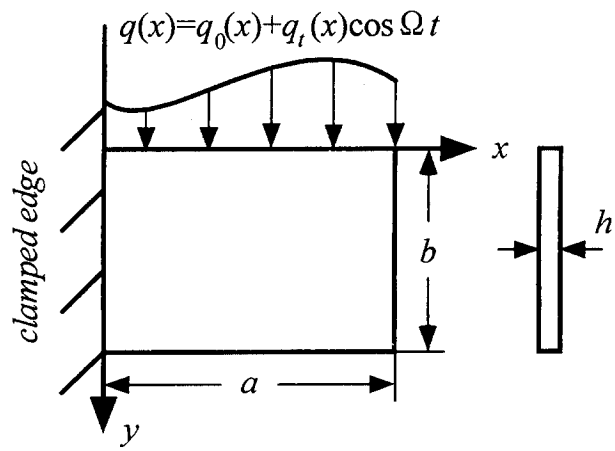

Fig. 1 Geometry of a cantilever plate

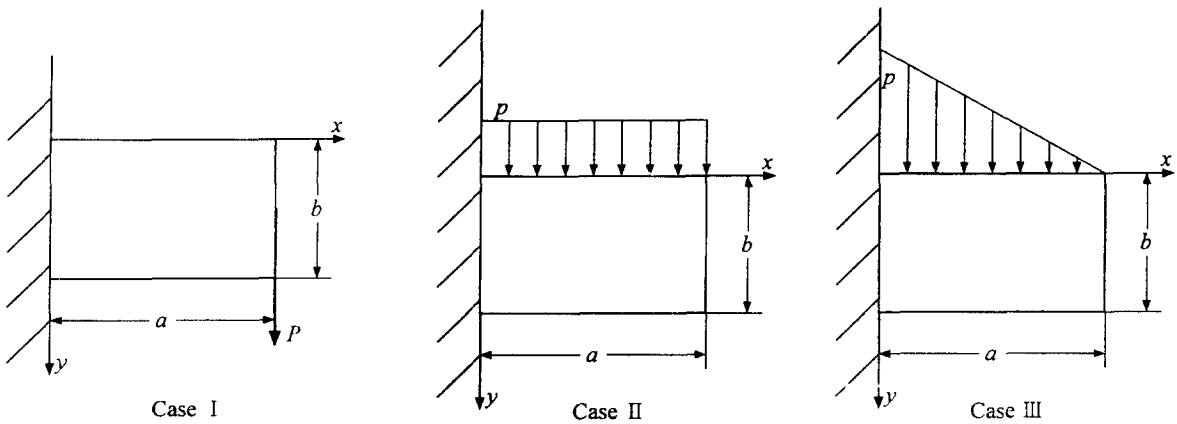

Case I Case II Case III

Fig. 2 In-plane force applied to the plate

$$U = \frac{1}{2}\iint_A \left[N_x \left(\frac{\partial w}{\partial x}\right)^2 + N_y \left(\frac{\partial w}{\partial y}\right)^2 + 2N_{xy} \left(\frac{\partial w}{\partial x}\right)\left(\frac{\partial w}{\partial y}\right) \right] dxdy \tag{3}$$

$$T = \frac{1}{2}\rho h \iint_A \left(\frac{\partial w}{\partial t}\right)^2 dxdy \tag{4}$$

where w denotes the transverse deflection, t is the time, $D=Eh^3/12(1-\nu^2)$ is the bending stiffness, E is Young's modulus, ν is the Poisson ratio, h is the plate thickness and ρ is the mass density.

The total potential energy can be written as

$$\Pi = V + U - T \tag{5}$$

3. Free vibration and buckling analysis

Free vibrations of a plate subjected to static force is given by setting p_t=0. The solution of the vibration problem which satisfies the geometric boundary conditions is assumed in the form

$$w = \sum_{m=1}^{N}\sum_{n=1}^{N} A_{mn}\, h_m(\xi)\, \bar{h}_n(\eta) e^{i\omega t} \tag{6}$$

where ω is the natural radian frequency, A_{mn} is an unknown constant, h_m is the vibration mode of the clamped-free beam, $\bar{h}_n$ is the vibration mode of the free-free beam, $\xi=x/a$ and $\eta=y/b$.

Applying the Rayleigh-Ritz method, i.e.,

$$\frac{\partial \Pi}{\partial A_{rs}} = 0 \tag{7}$$

in which r and s are 1, 2, $\cdots$, N gives the following set of algebraic equations

$$\sum_{m=1}\sum_{n=1} A_{mn}\,(E_{mrns} + \lambda_b \bar{p}_0 G_{mrns} - \lambda_v^4 F_{mrns}) = 0 \tag{8}$$

where $\lambda_v = \sqrt[4]{\rho h\,\omega^2 b^4/D}$ is the eigenvalue of vibration, λ_b is the eigenvalue of buckling (Case I: $\lambda_b = P_0 b^2/D$, Case II: $\lambda_b = p_0 hb^2/D$, Case III: $\lambda_b = p_0 hb^3/D$), $\bar{p}_0 = p_0/p_{cr}$ is the nondimensional static load, p_{cr} is the buckling load and E_{mrns}, G_{mrns} and F_{mrns} are constants depending on h_m, h_r, $\bar{h}_n$ and $\bar{h}_s$ (see Appendix B).

Eq. (8) can be put in matrix notation by using

$$([E] + \lambda_b \bar{p}_0 [G] - \lambda_v^4 [F])\{X\} = \{0\} \tag{9}$$

where $[E]$, $[G]$ and $[F]$ are the coefficient matrices, $e\{s+(r-1)N,\ n+(m-1)N\}=E_{mrns}$, $g\{s+(r-1)N,\ n+(\mathrm{m}-1)N\}=G_{mrns}$, $f\{s+(r-1)N,\ n+(\mathrm{m}-1)N\}=F_{mrns}$ and $\{X\}=\{A_{11}\ A_{12}\ \cdots\ A_{1N}\ \cdots\ A_{NN}\}^T$.

To obtain the eigenvalue λ_v in Eq. (9), one employs the method which obtains the eigenvalue of the matrix. If one puts $\lambda_v=0$ and $\bar{p}_0 = 1$, the equation for buckling eigenvalue λ_b is obtained.

4. Dynamic stability analysis

One can assume the solution of dynamic stability to be of the forms

$$w = \sum_{m=1}^{N}\sum_{n=1}^{N} T_{mn}(t)\,\overline{W}_{mn}(\xi,\ \eta) \tag{10}$$

in which T_{mn} is an unknown time function and $\overline{W}_{mn}$ is the vibration mode of the plate satisfying the geometric boundary conditions of the plate obtained by Eq. (6), defined as $\overline{W}_{mn} = \sum_{i=1} a_i^m h_i(\xi) \sum_{j=1} a_j^n \bar{h}_j(\eta)$.

Applying the Hamilton principle, one has

$$\delta \int_{t_1}^{t_2} (T - V - U)\,dt = 0 \tag{11}$$

where $\delta T_{mn}=0$ at $t=t_1$ and t_2.

After the indicated integrations, Eq. (11) gives a set of ordinary differential equations for the time variables

$$\sum_{m=1}\sum_{n=1}\sum_{k=1}\sum_{l=1}\left[C_{mn}^{kl}\ddot{T}_{mn} + \left\{ \frac{1}{k_{11}^4} A_{mn}^{kl} - \frac{\lambda_b}{k_{11}^4}(\bar{p}_0 + \bar{p}_t\cos\bar{\omega}\tau)\,B_{mn}^{kl} \right\} T_{mn} \right] = 0 \tag{12}$$

where $k_{11} = \sqrt[4]{\rho h\,\omega_{11}^2 b^4/D}$ is the first eigenvalue of vibration, $\bar{p}_t = p_t/p_{cr}$ is the nondimensional amplitude of the dynamic load, $\bar{\omega} = \Omega/\omega_{11}$ is the nondimensional excitation frequency, $\tau=\omega_{11}t$ is the nondimensional time, and C_{mn}^{kl}, A_{mn}^{kl} and B_{mn}^{kl} are constants depending on modes of vibration of the plate (see Appendix C).

Eq. (12) can be put in matrix notation by using

$$[C]\{\ddot{T}\}+[Q]\{T\}+(\bar{p}_0+\bar{p}_t\cos\bar{\omega}\tau)[R]\{T\}=\{0\} \tag{13}$$

where $[C]$, $[Q]$ and $[R]$ are the coefficient matrices, $c\{l+(k-1)L, n+(m-1)L\}=C_{mn}^{kl}$, $q\{l+(k-1)L, n+(m-1)L\}=\frac{1}{k_{11}^4}A_{mn}^{kl}$, $r\{l+(k-1)L, n+(m-1)L\}=\frac{\lambda_b}{k_{11}^4}B_{mn}^{kl}$ and $\{T\}=\{T_{11}\ T_{12}\cdots T_{1L}\ T_{21}\cdots T_{LL}\}^T$ is the column vector of the dependent variables.

By using the inverse matrix $[C]^{-1}$ and considering linear dampings, nondimensional form of the ordinary differential equations is then obtained as

$$[I]\{\ddot{T}\}+[H]\{\dot{T}\}+[F]\{T\}+(\bar{p}_0+\bar{p}_t\cos\bar{\omega}\tau)[G]\{T\}=0 \tag{14}$$

here $[I]$ is the unit matrix, $[H]=diag(2h_{ij}\omega_{ij})$ is the damping matrix, $[F]=[C]^{-1}[Q]=diag(\omega_{ij}^2)$ is the diagonal matrix and $[G]=[C]^{-1}[R]$ is the square matrix. h_{ij} is the damping constant and ω_{ij} is the nondimensional natural radian frequency with i-th mode number in the x direction and j-th mode number in the y direction in which $j=1, 3, \cdots$ corresponds to the symmetric mode of vibration and $j=2, 4, \cdots$ corresponds to the anti-symmetric mode of vibration.

The solution of Eq. (14) is now sought in the form (Takahashi 1982, 1981)

$$\{T\}=e^{\lambda\tau}\left\{\frac{1}{2}\boldsymbol{b}_0+\sum_{k=1}(\boldsymbol{a}_k\sin k\bar{\omega}\tau+\boldsymbol{b}_k\cos k\bar{\omega}\tau)\right\} \tag{15}$$

where $\boldsymbol{b}_0$, $\boldsymbol{a}_k$ and $\boldsymbol{b}_k$ are vectors that are independent of time variable and λ is an unknown constant.

Substitution of Eq. (15) into Eq. (14) and application of harmonic balance method yield a set of homogeneous algebraic equations

$$([M_0]-\lambda[M_1]-\lambda^2[M_2])\{X\}=\{0\} \tag{16}$$

where $[M_0]$, $[M_1]$ and $[M_2]$ are the coefficient matrices of the zeroth (constant), first and second powers of λ, respectively and $\{X\}$ is a column vector. Upon introducing the new variable $\{Y\}=\lambda\{X\}$, Eq. (16) becomes an eigenvalue problem of a double sized matrix

$$\begin{bmatrix}[0] & [I]\\ [M_2]^{-1}[M_0] & -[M_2]^{-1}[M_1]\end{bmatrix}\begin{Bmatrix}X\\ Y\end{Bmatrix}=\lambda\begin{Bmatrix}X\\ Y\end{Bmatrix} \tag{17}$$

As the matrix of Eq. (17) is a non-symmetric matrix with real elements, the eigenvalues consist of pairs of complex numbers. If the eigenvalues of the equation are distinct, then the necessary and sufficient condition for stability is that real parts of the complex roots should be negative or zero.

5. Basic properties of dynamic instability

There are two types of unstable motions obtained from Eq. (14): that is, simple parametric

resonance in the neighborhood of $\bar{\omega} = 2\omega_{ij}/q$ (q=1, 2, ⋯) and combination resonance in the neighborhood of $\bar{\omega} = (\omega_{ij} \pm \omega_{kl})/q$ (q=1, 2, ⋯), in which q=1, 2, ⋯ corresponds to the principal, second, ⋯ unstable regions.

The kind and width of the unstable regions depend on the elements of the matrix $[G]$. As the matrix $[G]$ is symmetric, combination resonances with sum type in the neighborhood of $\bar{\omega} = \omega_{ij} + \omega_{kl}$ will be obtained and combination resonances with difference type in the neighborhood of $\bar{\omega} = (\omega_{ij} - \omega_{kl})/q$ will not be obtained (Hsu 1963).

The coefficient matrix $[G]$ of the parametric excitation for the loading condition corresponding to case I has the following form if the first four modes of the symmetric and

$$[G] = \begin{bmatrix} 0 & 0 & 0 & 0 & g_{1211} & g_{2211} & g_{1411} & g_{3211} \\ 0 & 0 & 0 & 0 & g_{1221} & g_{2221} & g_{1421} & g_{3221} \\ 0 & 0 & 0 & 0 & g_{1213} & g_{2213} & g_{1413} & g_{3213} \\ 0 & 0 & 0 & 0 & g_{1223} & g_{2223} & g_{1423} & g_{3223} \\ g_{1112} & g_{2112} & g_{1312} & g_{2312} & 0 & 0 & 0 & 0 \\ g_{1122} & g_{2122} & g_{1322} & g_{2322} & 0 & 0 & 0 & 0 \\ g_{1114} & g_{2114} & g_{1314} & g_{2314} & 0 & 0 & 0 & 0 \\ g_{1132} & g_{2132} & g_{1332} & g_{2332} & 0 & 0 & 0 & 0 \end{bmatrix} \tag{18}$$

anti-symmetric vibrations are adopted

in this case, $\{T\}=\{T_{11}\ T_{21}\ T_{13}\ T_{23}\ T_{12}\ T_{22}\ T_{14}\ T_{32}\}^T$.

The time functions T_{11}, T_{21}, T_{13} and T_{23} have the symmetric modes, while the time functions T_{12}, T_{22}, T_{14} and T_{32} have the anti-symmetric modes.

The diagonal element g_{ijij} is zero as shown in Eq. (18). Parametric resonances occur only through the coupling term g_{ijkl} ($i \neq k$, $j \neq l$). Therefore, simple parametric resonance which occurs through the direct term g_{ijij} would not be important for the case I (Hsu 1963). Combination resonance which occurs through the non-zero coupling term is predominant. As the non-zero elements are g_{1112}, g_{2112}, g_{1312} and so on, combination resonances such as $\omega_{11}+\omega_{12}$, $\omega_{21}+\omega_{12}$, $\omega_{13}+\omega_{12}$, etc., would be included.

In the cases II and III, the matrix $[G]$ has non-zero elements. It is to be expected that the simple parametric resonances and combination resonances would be included simultaneously (Hsu 1963).

Based upon the preceding theoretical analysis, numerical solutions have been obtained for the cantilever rectangular plate. First, the natural frequencies and buckling load are presented. Then, the unstable regions are determined.

6. Buckling and vibration analysis

6.1. Accuracy of the solution

The ten-term solution of Eq. (8) (N=10) is used in the present free vibration and buckling analysis. The ten-term solution is converged and the present solution λ_v^2 for the square plate agrees well with the existing solution as shown in Table 1.

Table 1 Accuracy of the present solution

mode	present solution	existing solution
1st	3.484	3.494
2nd	8.521	8.547
3rd	21.38	21.44
4th	27.28	27.46
5th	31.07	31.17

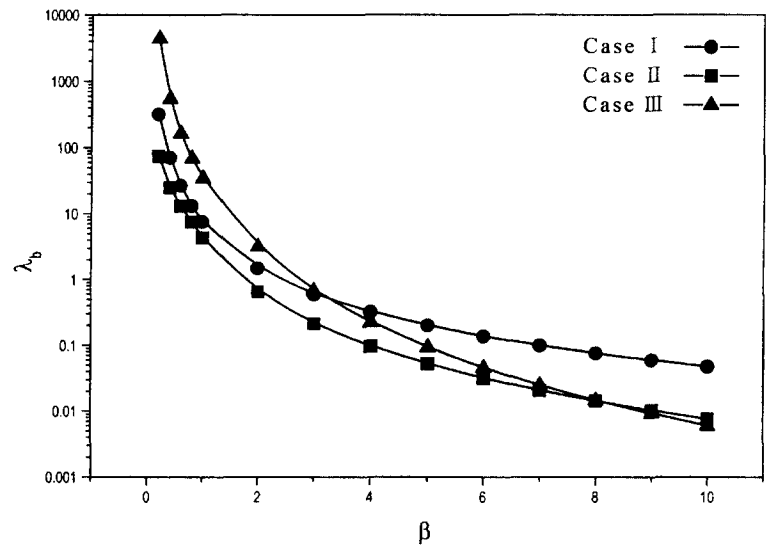

Fig. 3 Buckling curves of the rectangular plate

6.2. Buckling properties

Fig. 3 shows buckling curves of the rectangular plate for three different loading conditions. The buckling load decreases with increase of the aspect ratio β ($=a/b$). Fig. 4 shows buckling modes of the square plate. The deflection of the loaded end is large in the cases of distributed loads and the effect of the torsional mode is conspicuous. On the other hand, torsional mode and bending mode are the same order in the case I.

6.3. Comparison with the beam theory

Fig. 5 shows of the buckling curves obtained by the present analysis obtained by the plate theory and the beam theory (Japan 1971) in the case where $h=b/10$ and $\nu=0.3$. The ordinate λ_b denotes the buckling eigenvalue, while the abscissa β is the aspect ratio. The result of the present analysis coincides with the result obtained by the beam theory when the aspect ratio β is large. The accuracy of the present result seems to be satisfactory. When the aspect ratio β is less than 6.0, the difference between the plate theory and the beam theory is greater than 10%. The plate theory must be applied to the buckling analysis of the present problem.

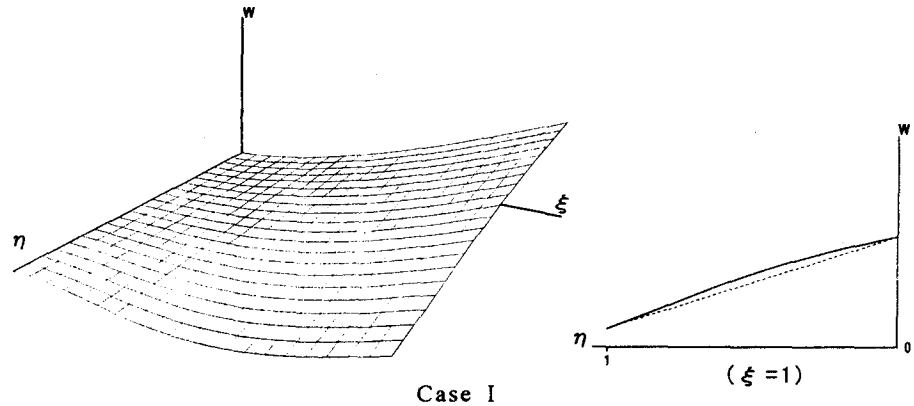

Case I

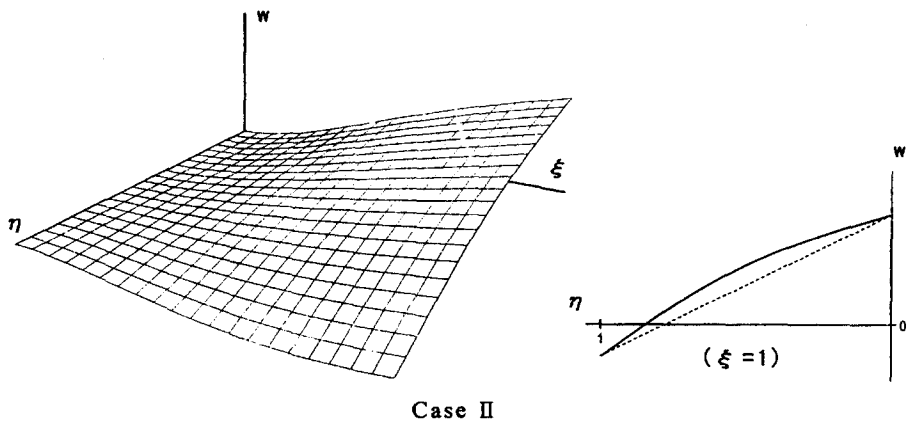

Case II

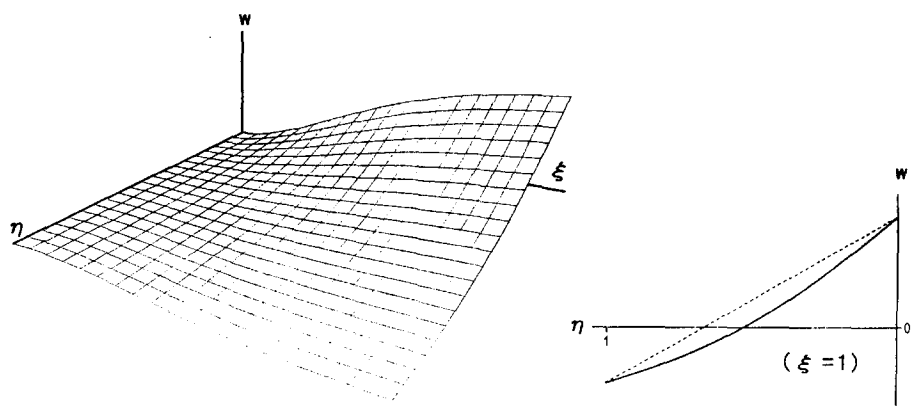

Case III

Fig. 4 Buckling mode of the square plate

6.4. Vibration analysis

The natural frequency versus the static load of the square plate for cases I, II and III are shown in Fig. 6. In these figures, the ordinate shows the nondimensional natural frequency,

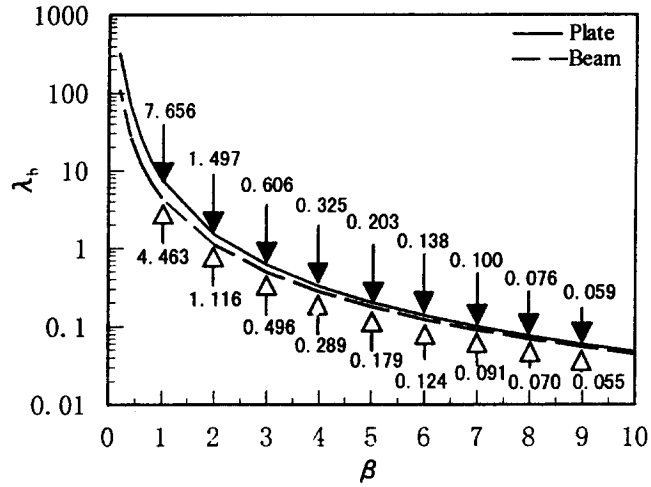

Fig. 5 Buckling curves of the plate and the beam theories

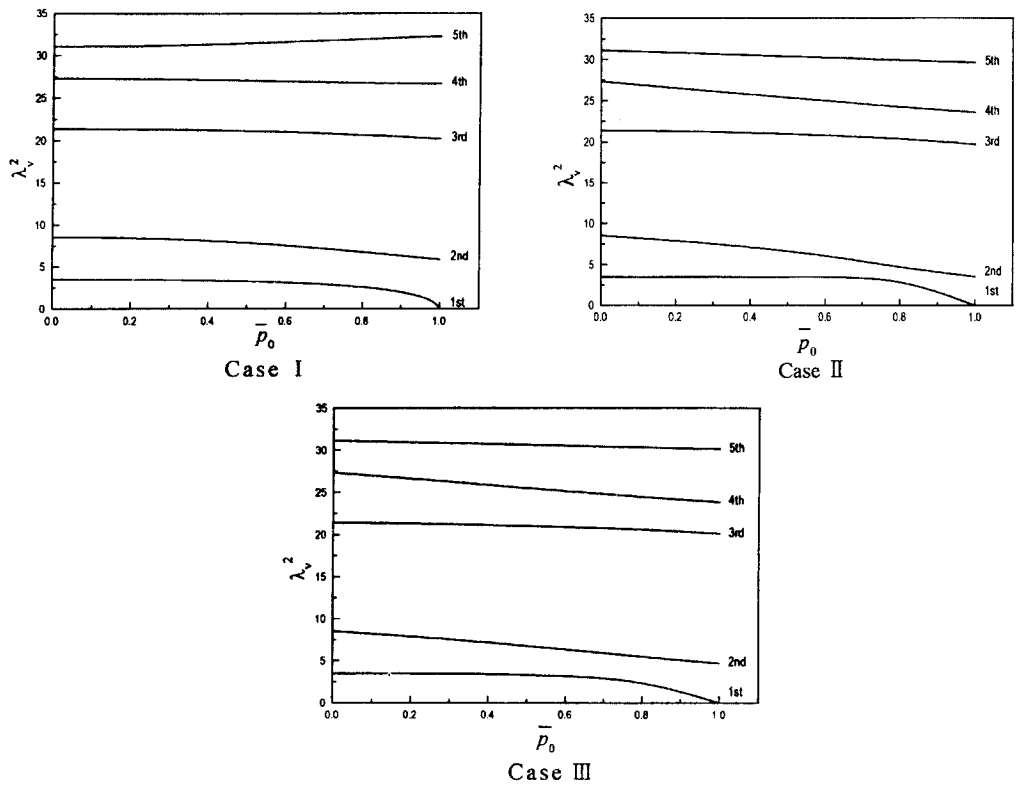

Fig. 6 Natural frequency vs. the static load

while the abscissa denotes the static load normalized to the buckling load in each case. Natural frequencies change with increase of the static load. Natural frequencies decrease with increase of the static load $\bar{p}_0$ except the fifth mode of the case I. The effect of the static load

is the most pronounced in the case of the first mode. In this case, the frequency is zero when the load $\bar{p}_0$ becomes unity. This result can be seen in structural mechanics. It is concluded that the present analysis is accurate. The mode of vibration of the first mode when the static load $\bar{p}_0$ is unity corresponds to that of buckling.

7. Dynamic stability analysis

7.1. Unstable regions of a square plate

The results of the square plate for different loading conditions with no static load $\bar{p}_0=0$ and undamped case ($h_{ij}=0$) are shown in Figs. 7 to 9. In these figures, the ordinate $\bar{p}_t$ denotes the amplitude of the periodic load normalized to the corresponding buckling load, while the abscissa $\bar{\omega}$ is the excitation frequency normalized to the lowest natural frequency. Further, the hatched portions represent the regions of various types of instability. The narrow regions of instability with $\bar{\omega}$ less than 0.2 when $\bar{p}_t=0.5$ are omitted in the figures. The three-term solution of Eq. (15) ($k=3$) is used in the present analysis. This solution is converged and agree well with stability boundaries obtained by the Runge-Kutta-Gill method.

Wide unstable regions of combination resonances of sum type in the vicinity of $\omega_{ij}+\omega_{kl}$ are obtained as shown in case I as shown in Fig. 7. As the diagonal elements of the coefficient matrix $[G]$ as shown in Eq. (18) are zero in the case I, the simple parametric resonance excited by the direct term is not obtained. However, the second unstable regions of the simple parametric resonance such as ω_{ij} occur through coupling terms. The widths of the simple parametric resonances are narrower than those of combination resonances. Therefore, combination resonances are important for the case I.

Simple parametric resonances with $2\omega_{12}$ and $2\omega_{13}$, etc. as well as combination resonances are obtained in cases II and III as shown in Figs. 8 and 9. The combination resonances are not predominant for cases II and III. From comparisons of Figs. 7 to 9, the force distribution along the edge of the plate can be seen to much affect the unstable regions.

7.2. Effect of static load

Fig. 10 shows undamped ($h_{ij}=0$) unstable regions of a square plate subjected to a static load $\bar{p}_0=0.5$ for the case I. Simple parametric resonances with the principal unstables regions such

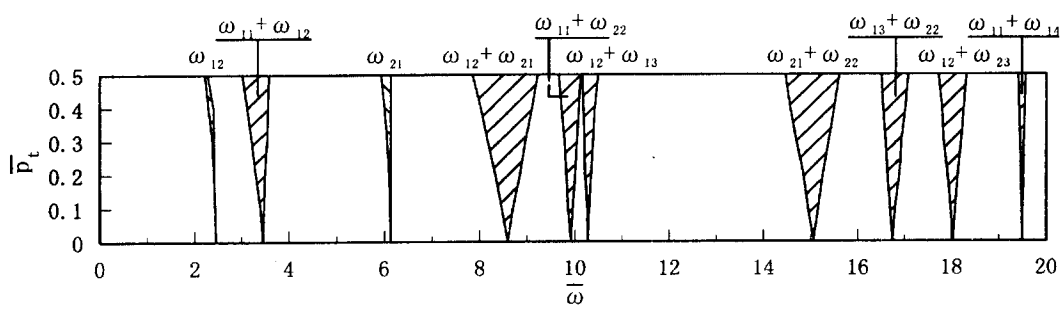

Fig. 7 Unstable regions: case I, $\beta=1$, $\bar{p}_0=0$ and $h_{ij}=0$

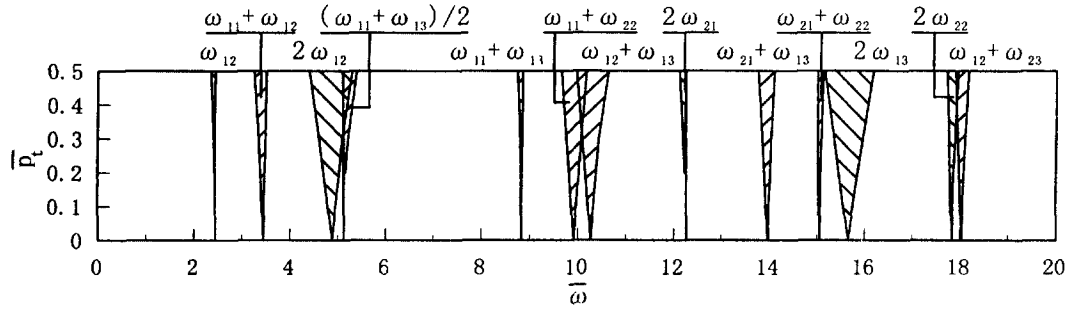

Fig. 8 Unstable regions: case II, β=1, $\bar{p}_0$=0 and h_{ij}=0

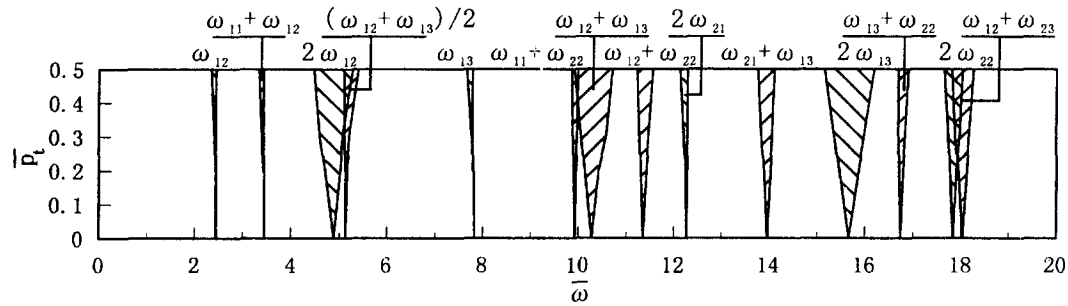

Fig. 9 Unstable regions: case III, β=1, $\bar{p}_0=0$ and h_{ij}=0

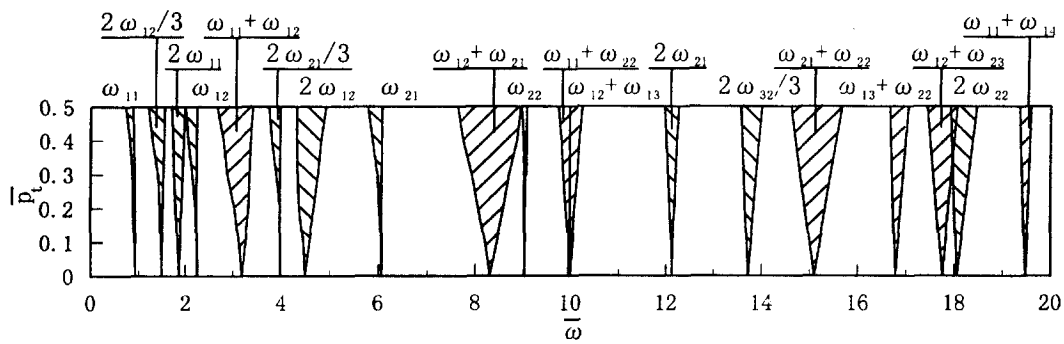

Fig. 10 Unstable regions: case I, β=1, $\bar{p}_0=0$ and h_{ij}=0

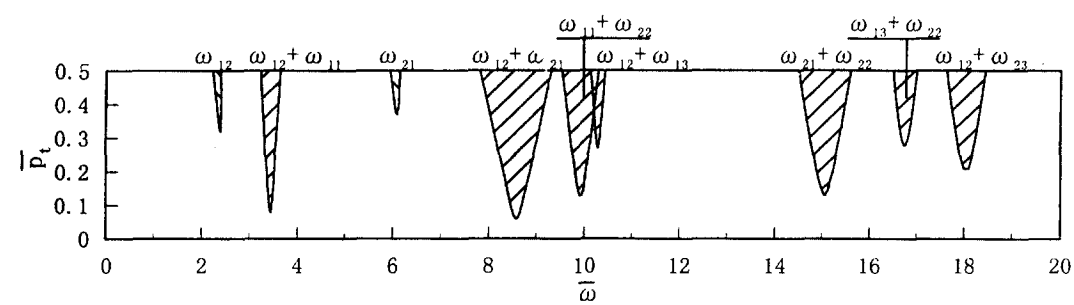

Fig. 11 Unstable regions: case I, β=1, $\bar{p}_0=0$ and h_{ij}=0.01

as $2\omega_{11}$, $2\omega_{12}$, $2\omega_{21}$ and $2\omega_{22}$ and the third unstable regions such as $2\omega_{12}/3$, $2\omega_{21}/3$ and $2\omega_{32}/3$ occur in conjunction with $\bar{p}_0$. This result corresponds to the fact that the coupling between the modes through the restoring force terms in Eq. (14). The static load $\bar{p}_0$ has an influence upon the unstable regions. The simple resonances of small width in the absence of the static load $\bar{p}_0$ become of larger width.

7.3. Effect of damping

Fig. 11 shows undamped (h_{ij}=0) and damped (h_{ij}=0.01) unstable regions of a square plate for case I. The effect of damping depends on the width of the unstable region and is to produce degeneracy of the unstable regions in the present case.

8. Conclusions

The dynamic stability of a rectangular cantilever plate subjected to in-plane load has been investigated. The conclusions are as follows.

(1) Combination resonances with sum type are predominant for a plate subjected to concentrated load along the free end. Simple parametric resonances and combination resonances are excited simultaneously for a plate subjected to distributed load. The stress distribution along the edge affects the kinds and widths of unstable regions.

(2) Static load has influence upon the kinds and widths of unstable region of a plate subjected to in-plane dynamic load. The simple resonances whose widths are narrow in the absence of a static load become broad in width.

References

Bolotin, V.V. (1964), *The Dynamic Stability of Elastic Systems*, Holden-Day.

Column Research Committee of Japan (1971), *Handbook of Structural Stability*, Corona, 1-112.

Hsu, C.H. (1963), "On the Parametric excitation of dynamic systems having multiple degree of freedom", *Journal of Applied Mechanics*, **30**, 363-372.

Leissa, A.W. (1969), *Vibration of Plates*, NASA, Sp-160, 76.

Takahashi, K. and Konishi, Y. (1988), "Dynamic stability of a rectangular plate subjected to distributed in-plane dynamic force", *Journal of Sound and Vibration*, **123**(1), 115-127.

Takahashi, K. (1982), "Instability of parametric dynamic systems with non-uniform damping", *Journal of Sound and Vibration*, **80**, 257-262.

Takahashi, K. (1981), "An approach to inuestigate the instability of the multiple-degree-of-freedom parametric dynamic systems", *Journal of Sound and Vibration*, **78**(4), 519-529.

Yamaki, N. and Nagai, K. (1975), "Dynamic stability of rectangular plates under periodic compressive forces", *Reports of the Institute of the High Speed Mechanics*, Tohoku University, **32**, 103-127.

Appendix A: In-plane forces, N_x, N_y and N_{xy}

Case I: concentrated load $P=P_0+P_t\cos\Omega t$ along the free end $x=a$

$$N_x = -\frac{12P}{b^3}(y - b/2)(a - x) \tag{A-1}$$

$$N_y = 0 \tag{A-2}$$

$$N_{xy} = -\frac{6P}{b^3}(y - b/2)^2 + \frac{3P}{2b} \tag{A-3}$$

Case II: uniformly distributed load $p=p_0+p_t\cos\Omega t$ along the free end $y=0$

$$N_x = -ph\left[6(a-x)^2\frac{(y-b/2)}{b^3} - \frac{b^2}{5}\left\{\frac{20(y-b/2)^3}{b^5} - \frac{3(y-b/2)}{b^3}\right\}\right] \tag{A-4}$$

$$N_y = -ph\left\{\frac{2(y-b/2)^3}{b^3} - \frac{3(y-b/2)}{2b} + \frac{1}{2}\right\} \tag{A-5}$$

$$N_{xy} = ph(a-x)\left\{\frac{6(y-b/2)^2}{b^3} - \frac{3}{2b}\right\} \tag{A-6}$$

Case III: triangularly distributed load $p=p_0(1-x/a)+p_t(1-x/a)\cos\Omega t$ along the free end $y=0$

$$N_x = ph\left\{\frac{2(a-x)^3(b/2-y)}{b^3} - \frac{4(a-x)(b/2-y)^3}{b^3} + \frac{3(a-x)(b/2-y)}{5b}\right\} \tag{A-7}$$

$$N_y = ph\left\{-\frac{3(a-x)(b/2-y)}{2b} + \frac{2(a-x)(b/2-y)^3}{b^3} - \frac{a-x}{2}\right\} \tag{A-8}$$

$$N_{xy} = -ph\left\{-\frac{3(a-x)^2}{4b} + \frac{(3a-x)^2(b/2-y)^2}{b^3} - \frac{b}{80} - \frac{(b/2-y)^4}{b^3} + \frac{3(b/2-y)^2}{10b}\right\} \tag{A-9}$$

Appendix B: Coefficient, E_{mrns}, F_{mrns} and G_{mrns}

$$E_{mrns} = \frac{1}{\beta^4} I_{mr}^2 \bar{I}_{ns}^1 + I_{mr}^1 \bar{I}_{ns}^2 + \frac{\nu}{\beta^2}(I_{mr}^3 \bar{I}_{ns}^4 + I_{mr}^4 \bar{I}_{ns}^3) + \frac{2(1-\nu)}{\beta^2} I_{mr}^5 \bar{I}_{ns}^5 \tag{B-1}$$

$$F_{mrns} = I_{mr}^1 \bar{I}_{ns}^1 \tag{B-2}$$

$$G_{mrns} = -\frac{3}{2\beta}\{8I_{mn}^6 \bar{I}_{ns}^6 + 4(I_{mn}^7 \bar{I}_{ns}^{10} + I_{mn}^8 \bar{I}_{ns}^9) - (I_{mn}^7 \bar{I}_{ns}^8 + I_{mn}^8 \bar{I}_{ns}^7)\}$$

for case I

$$G_{mrns} = -6I_{mn}^9 \bar{I}_{ns}^6 - \frac{4}{\beta^2} I_{mn}^5 \bar{I}_{ns}^{11} - \frac{3}{5\beta^2} I_{mn}^5 \bar{I}_{ns}^6 - 2I_{mn}^1 \bar{I}_{ns}^{13} + \frac{3}{2} I_{mn}^1 \bar{I}_{ns}^{12} - \frac{1}{2} I_{mn}^1 \bar{I}_{ns}^5 \tag{B-3}$$

$$+ 6(I_{mn}^{10} \bar{I}_{ns}^{10} + I_{mn}^{11} \bar{I}_{ns}^9) - \frac{3}{2}(I_{mn}^{10} \bar{I}_{ns}^8 + I_{mn}^{11} \bar{I}_{ns}^7)$$

for case II

$$G_{mrns} = -2\beta I_{mr}^{12}\bar{I}_{ns}^{6} + \frac{4}{\beta} I_{mr}^{6}\bar{I}_{ns}^{11} - \frac{3}{\beta} I_{mr}^{6}\bar{I}_{ns}^{6} + \frac{3}{2}\beta I_{mr}^{13}\bar{I}_{ns}^{12} + 2\beta I_{mr}^{13}\bar{I}_{ns}^{13} - \frac{\beta}{2} I_{mr}^{13}\bar{I}_{ns}^{5}$$
$$+ \frac{3}{8}\beta(I_{mr}^{14}\bar{I}_{ns}^{8} + I_{mr}^{15}\bar{I}_{ns}^{7}) + \frac{3}{2}\beta(I_{mr}^{14}\bar{I}_{ns}^{10} + I_{mr}^{15}\bar{I}_{ns}^{9}) + \frac{1}{160\beta}(I_{mr}^{7}\bar{I}_{ns}^{8} + I_{mr}^{8}\bar{I}_{ns}^{7})$$
$$+ \frac{1}{2\beta}(I_{mr}^{7}\bar{I}_{ns}^{15} + I_{mr}^{8}\bar{I}_{ns}^{14}) - \frac{3}{20\beta}(I_{mr}^{7}\bar{I}_{ns}^{10} + I_{mr}^{8}\bar{I}_{ns}^{9})$$

for case III

where

$$I_{mr}^{1} = \int_0^1 h_m h_r \, d\xi \qquad \bar{I}_{ns}^{1} = \int_0^1 \bar{h}_n \bar{h}_s \, d\eta$$
$$I_{mr}^{2} = \int_0^1 h_{2m} h_{2r} \, d\xi \qquad \bar{I}_{ns}^{2} = \int_0^1 \bar{h}_{2n} \bar{h}_{2s} \, d\eta$$
$$I_{mr}^{3} = \int_0^1 h_{2m} h_r \, d\xi \qquad \bar{I}_{ns}^{3} = \int_0^1 \bar{h}_{2n} \bar{h}_s \, d\eta$$
$$I_{mr}^{4} = \int_0^1 h_m h_{2r} \, d\xi \qquad \bar{I}_{ns}^{4} = \int_0^1 \bar{h}_n \bar{h}_{2s} \, d\eta$$
$$I_{mr}^{5} = \int_0^1 h_{1m} h_{1r} \, d\xi \qquad \bar{I}_{ns}^{5} = \int_0^1 \bar{h}_{1n} \bar{h}_{1s} \, d\eta$$
$$I_{mr}^{6} = \int_0^1 (1-\xi) h_{1m} h_{1r} \, d\xi \qquad \bar{I}_{ns}^{6} = \int_0^1 (1-2\eta) \bar{h}_n \bar{h}_s \, d\eta$$
$$I_{mr}^{7} = \int_0^1 h_{1m} h_r \, d\xi \qquad \bar{I}_{ns}^{7} = \int_0^1 \bar{h}_{1n} \bar{h}_s \, d\eta$$
$$I_{mr}^{8} = \int_0^1 h_m h_{1r} \, d\xi \qquad \bar{I}_{ns}^{8} = \int_0^1 \bar{h}_n \bar{h}_{1s} \, d\eta$$
$$I_{mr}^{9} = \int_0^1 (1-\xi)^2 h_{1m} h_{1r} \, d\xi \qquad \bar{I}_{ns}^{9} = \int_0^1 (1-2\eta)^2 \bar{h}_{1n} \bar{h}_s \, d\eta$$
$$I_{mr}^{10} = \int_0^1 (1-\xi) h_{1m} h_r \, d\xi \qquad \bar{I}_{ns}^{10} = \int_0^1 (1-2\eta)^2 \bar{h}_n \bar{h}_{1s} \, d\eta$$
$$I_{mr}^{11} = \int_0^1 (1-\xi) h_m h_{1r} \, d\xi \qquad \bar{I}_{ns}^{11} = \int_0^1 (1-2\eta)^3 \bar{h}_n \bar{h}_s \, d\eta$$
$$I_{mr}^{12} = \int_0^1 (1-\xi)^3 h_{1m} h_{1r} \, d\xi \qquad \bar{I}_{ns}^{12} = \int_0^1 (1-2\eta) \bar{h}_{1n} \bar{h}_{1s} \, d\eta$$
$$I_{mr}^{13} = \int_0^1 (1-\xi) h_m h_r \, d\xi \qquad \bar{I}_{ns}^{13} = \int_0^1 (1-2\eta)^3 \bar{h}_{1n} \bar{h}_{1s} \, d\eta$$
$$I_{mr}^{14} = \int_0^1 (1-\xi)^2 h_{1m} h_r \, d\xi \qquad \bar{I}_{ns}^{14} = \int_0^1 (1-2\eta)^4 \bar{h}_{1n} \bar{h}_s \, d\eta$$
$$I_{mr}^{15} = \int_0^1 (1-\xi)^2 h_m h_{1r} \, d\xi \qquad \bar{I}_{ns}^{15} = \int_0^1 (1-2\eta)^4 \bar{h}_n \bar{h}_{1s} \, d\eta$$

$$h_{1m} = \frac{dh_m}{d\xi}, \quad h_{2m} = \frac{d^2 h_m}{d\xi^2}, \cdots.$$

Appendix C: Coefficients, A_{mn}^{kl}, B_{mn}^{kl} and C_{mn}^{kl}

$$A_{mn}^{kl} = \int_0^1\int_0^1 \left\{ \frac{1}{\beta^4} \bar{W}_{mn,\xi\xi}\bar{W}_{kl,\xi\xi} + \bar{W}_{mn,\eta\eta}\bar{W}_{kl,\eta\eta} \right.$$
$$\left. + \frac{\nu}{\beta^2}(\bar{W}_{mn,\xi\xi}\bar{W}_{kl,\eta\eta} + \bar{W}_{mn,\eta\eta}\bar{W}_{kl,\xi\xi}) + \frac{2(1-\nu)}{\beta^2} \bar{W}_{mn,\xi\eta}\bar{W}_{kl,\xi\eta} \right\} d\xi d\eta \qquad \text{(C-1)}$$

$$B_{mn}^{kl} = -\frac{3}{2\beta}\int_0^1\int_0^1 \left[8(1-\xi)\left(\eta-\frac{1}{2}\right)\overline{W}_{mn,\xi}\overline{W}_{kl,\xi} + \left\{4\left(\eta-\frac{1}{2}\right)^2 - 1\right\}(\overline{W}_{mn,\xi}\overline{W}_{kl,\eta} + \overline{W}_{kl,\eta}\overline{W}_{mn,\xi}\right] d\xi d\eta$$

for case I

$$\begin{aligned} B_{mn}^{kl} = \int_0^1\int_0^1 \Bigg[& \left\{-6(1-\xi)^2\left(\eta-\frac{1}{2}\right) + \frac{4}{\beta^2}\left(\eta-\frac{1}{2}\right)^3 - \frac{3}{5\beta^2}\left(\eta-\frac{1}{2}\right)\right\}\overline{W}_{mn,\xi}\overline{W}_{kl,\xi} \\ & + \left\{-2\left(\eta-\frac{1}{2}\right)^3 + \frac{3}{2}\left(\eta-\frac{1}{2}\right) - \frac{1}{2}\right\}\overline{W}_{mn,\eta}\overline{W}_{kl,\eta} \\ & + \left\{6(1-\xi)\left(\eta-\frac{1}{2}\right)^3 - \frac{3}{2}(1-\xi)\right\}(\overline{W}_{mn,\xi}\overline{W}_{kl,\eta} + \overline{W}_{kl,\eta}\overline{W}_{mn,\xi})\Bigg] d\xi d\eta \end{aligned} \tag{C-2}$$

for case II

$$\begin{aligned} B_{mn}^{kl} = \int_0^1\int_0^1 \Bigg[& \left\{-2\beta(1-\xi)^3\left(\eta-\frac{1}{2}\right) + \frac{4}{\beta}(1-\xi)\left(\eta-\frac{1}{2}\right)^3 - \frac{3}{\beta}(1-\xi)\left(\eta-\frac{1}{2}\right)\right\}\overline{W}_{mn,\xi}\overline{W}_{kl,\xi} \\ & + \left\{-\frac{3}{2}\beta(1-\xi)\left(\eta-\frac{1}{2}\right) - 2\beta(1-\xi)\left(\eta-\frac{1}{2}\right)^3 - \frac{1}{2}\beta(1-\xi)\right\}\overline{W}_{mn,\eta}\overline{W}_{kl,\eta} \\ & + \Bigg\{\frac{3}{8}\beta(1-\xi)^2 + \frac{3}{2}\beta(1-\xi)^2\left(\eta-\frac{1}{2}\right)^2 + \frac{1}{160\beta} \\ & + \frac{1}{2\beta}\left(\eta-\frac{1}{2}\right)^4 + \frac{3}{20\beta}\left(\eta-\frac{1}{2}\right)^2\Bigg\}(\overline{W}_{mn,\xi}\overline{W}_{kl,\eta} + \overline{W}_{kl,\eta}\overline{W}_{mn,\xi})\Bigg] d\xi d\eta \end{aligned}$$

for case III

$$C_{mn}^{kl} = \int_0^1\int_0^1 \overline{W}_{mn,\xi}\overline{W}_{kl,\eta} d\xi d\eta \tag{C-3}$$

where $\overline{W}_{uv} = \sum_{m=1} a_m^u h_m \sum_{n=1} a_n^v \overline{h}_n$, $\overline{W}_{uv,\xi\eta} = \sum_{m=1} a_m^u h_{1m} \sum_{n=1} a_n^v \overline{h}_{1n}$, $\overline{W}_{uv,\xi\xi} = \sum_{m=1} a_m^u h_{2m} \sum_{n=1} a_n^v \overline{h}_n$,

$\overline{W}_{uv,\eta\eta} = \sum_{m=1} a_m^u h_m \sum_{n=1} a_n^v \overline{h}_{2n}$, $\overline{W}_{uv,\xi} = \sum_{m=1} a_m^u h_{1m} \sum_{n=1} a_n^v \overline{h}_n$, $\overline{W}_{uv,\eta} = \sum_{m=1} a_m^u h_m \sum_{n=1} a_n^v \overline{h}_{1n}$.